

Published in final edited form as:

*Nat Metab.* 2020 November 01; 2(11): 1223–1231. doi:10.1038/s42255-020-00276-5.

## Mitochondrial pyruvate carrier abundance mediates pathological cardiac hypertrophy

Mariana Fernandez-Caggiano<sup>1,\*</sup>, Alisa Kamynina<sup>1</sup>, Asvi A. Francois<sup>1</sup>, Oleksandra Pryszyzna<sup>1</sup>, Thomas R. Eykyn<sup>2</sup>, Susanne Krasemann<sup>3</sup>, Maria G. Crespo-Leiro<sup>4,5</sup>, Maria Garcia Vieites<sup>4</sup>, Katuscia Bianchi<sup>6</sup>, Valle Morales<sup>6</sup>, Nieves Domenech<sup>4,5</sup>, Philip Eaton<sup>1,\*</sup>

<sup>1</sup>The William Harvey Research Institute, Charterhouse Square, Barts and the London School of Medicine and Dentistry, Queen Mary University of London, London EC1M 6BQ

<sup>2</sup>School of Biomedical Engineering & Imaging Sciences, King's College London, London, UK

<sup>3</sup>University Medical Center Hamburg Eppendorf UKE. Institute for Neuropathology Research Campus N27, Hamburg, Germany

<sup>4</sup>Unidad de Cirugía Cardíaca y Trasplante, Servicio de Cardiología, Complejo Hospitalario Universitario de A Coruña (CHUAC), Instituto de Investigación Biomédica de A Coruña (INIBIC), A Coruña, Spain

<sup>5</sup>Centro de Investigación Biomédica en Red de Enfermedades Cardiovasculares (CIBERCV), Madrid, Spain

<sup>6</sup>Barts Cancer Institute, Queen Mary, John Vane Science Centre, University of London, Charterhouse Square, London EC1M 6BQ, UK

### Abstract

Cardiomyocytes rely on metabolic substrates, not only to fuel cardiac output, but also for growth and remodeling during stress. Here we show that Mitochondrial Pyruvate Carrier (MPC) abundance mediates pathological cardiac hypertrophy. MPC abundance was reduced in failing hypertrophic human hearts, as well as the myocardium of mice induced to fail by angiotensin II or transverse-aortic constriction-induced. Constitutive knockout of cardiomyocyte MPC1/2 in mice resulted in cardiac hypertrophy and reduced survival, while tamoxifen-induced cardiomyocyte-specific reduction of MPC1/2 to the attenuated levels observed during pressure-overload was sufficient to induce hypertrophy with impaired cardiac function. Failing hearts from cardiomyocyte-restricted knockout mice displayed increased abundance of anabolic metabolites, including amino acids and pentose phosphate pathway intermediates and reducing cofactors.

---

Users may view, print, copy, and download text and data-mine the content in such documents, for the purposes of academic research, subject always to the full Conditions of use: [http://www.nature.com/authors/editorial\\_policies/license.html#terms](http://www.nature.com/authors/editorial_policies/license.html#terms)

\*Correspondence to: m.f.caggiano@qmul.ac.uk or p.eaton@qmul.ac.uk.

#### Author Contributions

P.E. and M.F.C. conceived the project. M.F.C., A.K., A.A.F. and O.P. conducted experiments. S.K. performed histology. K.B. and V.M. conducted the C13 flux metabolomics using LC-MS analysis. N.D., M.G.C.L., M.G.V. collected human tissue samples and clinical data. M.F.C. and T.R.E. analysed the metabolomic data. P.E. and M.F.C. wrote the manuscript. All authors discussed the results and reviewed the manuscript.

#### Competing interests

The authors declare no competing interests.

These hearts showed a concomitant decrease in carbon flux into mitochondrial tricarboxylic acid cycle intermediates, as corroborated by complementary 1,2-<sup>13</sup>C<sub>2</sub>-glucose tracer studies. In contrast, inducible cardiomyocyte overexpression of MPC1/2 resulted in increased tricarboxylic acid cycle intermediates, and sustained carrier expression during transverse-aortic constriction protected against cardiac hypertrophy and failure. Collectively, we demonstrate that loss of the MPC1/2 causally mediates adverse cardiac remodelling.

---

Healthy myocardial mitochondria primarily utilise oxidative phosphorylation to generate adenosine triphosphate (ATP), which is required to meet the heart's energy-demanding function as a blood pump. In healthy myocardium with sufficient oxygen supply, oxidation of fatty acids provides approximately 60-90% of myocardial acetyl-CoA that contributes to ATP generation, with 10-40% arising from pyruvate oxidation<sup>1,2</sup>. However, the stressed human heart changes its fuel preference<sup>3,4</sup>, switching from fatty acids to glucose as a favoured carbon source<sup>5,6</sup>. Consistent with this observation, several studies with animal models of pressure-overload-induced hypertrophy have shown reduced fatty acid oxidation rates with enhanced glucose uptake and glycolysis accompanied with a compensatory anaplerosis to maintain the tricarboxylic acid cycle flux in the pathological heart<sup>7-9</sup>. Interestingly, this enhanced glycolysis and carbon influx via anaplerosis did not augment ATP production, consistent with an 'uncoupling' between glycolysis and glucose oxidation during pathological hypertrophy<sup>7,10,11</sup>. Furthermore, instead of pyruvate predominantly being oxidised in the mitochondria, it is metabolised by alternate pathways, including reductive fermentation to lactate despite sufficient oxygen availability<sup>12,13</sup>. This is reminiscent of the Warburg effect whereby many cancer cells increase glucose uptake and convert it to lactate via the reduction of pyruvate despite oxygen availability.

Since the identification of the mitochondrial pyruvate carrier (MPC) in 2012<sup>14,15</sup> several studies reported its role in cell growth and proliferation<sup>16-18</sup>. Mammalian MPC comprises two subunits, MPC1 and MPC2, with the absence of either attenuating mitochondrial pyruvate uptake<sup>14,15</sup>. Overexpression of MPC in cancer cells profoundly limited their growth, including in spheroid or xenograft-implantation models, whereas decreased expression promoted migration, chemotherapy resistance and reduced patient survival<sup>19-22</sup>. Overall this makes a compelling case that decreased MPC abundance may causatively contribute to the Warburg effect and the associated growth potentiation. Consistent with this rationale, we hypothesised that the decreased expression of MPC we observed in hearts from humans or mice with hypertrophic cardiomyopathy, may underlie the switch to anabolism that culminates in maladaptive hypertrophic growth and failure.

Western blot analysis of human hypertrophic cardiomyopathic hearts showed decreased MPC1/2 expression compared to control tissue (Fig. 1a). Administration of pro-hypertrophic angiotensin II to mice for 3-days significantly reduced cardiac MPC1 and MPC2 expression, which remained low 14-days after treatment initiation (Fig. 1b, Extended Data Fig. 1a). MPC expression was similarly attenuated in hearts subjected to cardiac pressure overload involving surgically-induced transverse aortic constriction (TAC) for 21-days that induced hypertrophy (Fig. 1c, Extended Data Fig. 1b).

To investigate whether decreased MPC1/2 expression was casual in the development of cardiac hypertrophy, we developed cardiomyocyte-specific MPC1 or MPC2 transgenic mice models in which we can increase or decrease the expression of either subunit. However, although the transgenic lines were designed so that MPC1 or MPC2 expression can be individually altered, we found as others have<sup>19,23</sup>, that increasing or decreasing one subunit resulted in a concomitant matched change in the other.

Knockout of cardiomyocyte MPC1 or MPC2 separately from birth resulted in complete loss of the other subunit and induced robust heart hypertrophy (Fig. 2a and 2b). A limitation of studying MPC1 or MPC2 KO mice was their high rate of mortality from 5-6 weeks of age (Fig. 2c). Real-time PCR analysis showed the cardiac hypertrophy markers atrial natriuretic peptide (ANP) and brain natriuretic peptide (BNP) were significantly increased in MPC1 KO as well as the partial MPC1 (*MPC1*<sup>-/+</sup>) mice, whereas  $\beta$ -myosin heavy chain ( $\beta$ -MHC) was significantly increased only in the MPC1 KO mice (Fig. 2d). Partial knockdown of MPC1 from birth to the levels observed in TAC- or angiotensin II-induced hypertrophy, also resulted in heart hypertrophy and failure (Fig. 2e, Extended Data Fig. 2).

The observations presented above supported a causal role for decreased MPC abundance in the progression of hypertrophy and heart failure, but the lifelong, constitutive decrease in MPC1/2 expression in the mice studied was a concern. Consequently, we generated a transgenic line (*TAXMPC1*), in which cardiomyocyte MPC1/2 abundance was inducibly decreased by administering tamoxifen once mice reached adulthood. In these mice, an intraperitoneal administration of tamoxifen promoted the activation of Cre recombinase with the consequent excision of the first exon of the MPC1 gene from the F.A.S.T cassette only in cardiac myocytes (Fig. 3a). Homozygous (*TAXMPC1* KO) or heterozygous (*TAXMPC1*<sup>+/-</sup>) mice for the F.A.S.T cassette showed similar MPC1 and MPC2 protein expression to its respective control (*Mhy6Cre*) in the absence of tamoxifen administration (Fig. 3b). 10-days after tamoxifen injection, the protein expression levels of both subunits were markedly decreased in *TAXMPC1* KO and partially decreased in the *TAXMPC1*<sup>+/-</sup> line (Fig. 3c). Immunofluorescence analyses of dystrophin expression in heart sections confirmed cardiac myocyte hypertrophy in *TAXMPC1*<sup>+/-</sup> mice compared to *Mhy6Cre* controls 21-days after the initiation of tamoxifen treatment (Extended Data Fig. 4). Cardiac MPC expression in *TAXMPC1*<sup>+/-</sup> mice mimicked the loss observed in angiotensin II- or TAC-treated hearts and this induced-reduction in adult mice was alone sufficient to promote hypertrophy. These hearts had high mRNA expression of the hypertrophic markers BNP, ANP and  $\beta$ -MHC (Fig. 3d), a significant increase in heart weight/tibia length ratio (Figure 3e), a deterioration in ejection fraction (Fig. 3f), and impaired left ventricular function as illustrated by a reduction by fractional shortening (Fig. 3g). These observations further substantiate that decreased expression of MPC1/2 causatively mediates myocardial growth and progression to heart failure.

Whilst the hypertrophic heart shows enhanced utilisation of glucose<sup>9</sup>, its oxidation is unaltered or decreases<sup>10,24,25</sup>. We hypothesised that decreased MPC expression during hypertrophy may causally mediate this ‘uncoupling’ of glycolysis from glucose oxidation. Indeed, we speculated that loss of MPC directly rewires metabolism to induce hypertrophic remodelling of the stressed myocardium. To test this hypothesis, hearts in which MPC1/2

was inducibly-decreased were compared to those with normal, control levels of the carrier using metabolomics profiling by mass spectrometry. This analysis showed glucose-derived carbon was rerouted, with impaired entry of pyruvate to mitochondria in hearts with less MPC1/2 (Fig. 3h and Supplementary Table 1). Consistent with this, all citric acid cycle intermediates were also less abundant, with decreases in citrate and aconitate reaching statistical significance. Intermediates of glycolysis were also reduced in hearts with low MPC1/2 compared to their respective controls, but pyruvate was concomitantly highly increased (Figure 3h). This increased pyruvate is consistent with impaired entry to the citric acid cycle and not because of enhanced glycolysis. The decrease in glycolytic intermediates was accompanied by its rerouting into the pentose phosphate pathway (PPP), as reflected by significant increases in 6-phosphoglycerate and sedoheptulose 7-phosphate, with ribulose 5-phosphate and ribose 5-phosphate also increasing - albeit not with significance (Fig. 3h). The PPP generates reduced nicotinamide adenine dinucleotide phosphate (NADPH), which is required for fatty acid and membrane biosynthesis, was also increased in the MPC KO mice (Fig. 3i). Similarly, 5-carbon ribose 5-phosphate required for nucleotide and nucleic acid production in the hypertrophying heart was increased<sup>26,27</sup>. We performed metabolomic flux tracer analysis of hearts from mice intravenously injected with 1,2-<sup>13</sup>C<sub>2</sub>-glucose to independently assess, based on the rationale depicted in Extended Data Fig. 5, whether glucose is rerouted to the PPP in myocardium with decreased MPC expression. Indeed, lactate and pyruvates derived from PPP, evidenced by them being singly <sup>13</sup>C-labelled, were significantly increased in TAXMPC1<sup>+/-</sup> hearts, consistent with rerouting of carbon from glucose into this pathway. Hearts with decreased MPC also concomitantly accumulated more doubly labelled pyruvate and lactate as a result of pyruvate not being incorporated inside the mitochondria and being reduced to lactate (Extended Data Fig. 5). This situation might be explained by a decrease in citric acid cycle metabolite abundance inside the mitochondria (Fig. 3h). Both shunting of glucose-derived carbon into the anabolic PPP and decreased incorporation of pyruvate into the tricarboxylic acid cycle of hearts with decreased MPC provides a rational explanation for the ‘uncoupling’ of glycolysis from glucose oxidation in the hypertrophic heart<sup>10,24,25</sup>. Furthermore, knockdown hearts had significantly more erythrose 4-phosphate, which couples to aromatic amino acids biosynthesis, explaining the significantly higher phenylalanine and tyrosine in these samples. Additional evidence that reducing pyruvate entry to the mitochondria promotes cardiac growth through enhanced PPP activity came from studies exposing H9C2 cardiomyoblasts to the MPC inhibitor UK5099, which enhanced growth and increased NADPH levels (Extended Data Fig. 6). Although UK5099 has a Ki for the MPC <50 nM, we used 10 or 20 μM based on previous work<sup>28</sup>. Furthermore, we knew from our study with isolated hearts<sup>29</sup> or others exposing cells to μM UK5099 that this did not cause toxicity or cell death. ATP and adenylate energy charge in tamoxifen-induced MPC KO hearts 10 days after carrier deletion were the same as in control tissue (Fig. 3h). This is notable, as it demonstrates that the metabolic remodelling that occurs in the hearts of mice with lower MPC1/2 level occurs independently of ATP abundance (Fig. 3h and Supplementary Table 1). This is consistent with the changes in metabolism upon MPC ablation causatively rerouting glucose carbon into biosynthetic pathways to provide the diverse array of substrates required for myocardial growth. However, additional mechanisms, including those arising from changes in cytosolic redox that occur because of the altered lactate/pyruvate ratio (Fig. 3h)

or alterations to pyruvate dehydrogenase activity may contribute to the remodelling. Ideally we would have performed metabolomics on myocardium from WT mice under control as well as TAC conditions, but we did not because of limited resources and because several studies already reported on this<sup>30</sup>.

If decreased MPC1/2 is critical for cardiac hypertrophy and not simply a bystander effect, maintaining carrier expression should rescue the aberrant growth phenotype. To address this possibility, as explained below, we generated transgenic mice that allowed MPC1/2 expression to be inducibly-maintained at healthy heart levels during stress that otherwise culminates in loss of carrier expression and hypertrophy.

We generated tAMPC1 as well as tAMPC2 cardiomyocyte-specific transgenic mouse lines in which doxycycline removal inducibly increases carrier expression. Cardiac specific tetracycline *trans*-activator (tTA) transcription factor interacts very efficiently with the tetO promoter in the absence of doxycycline and induces the transcription of MPC (Fig. 4a). MPC1 over-expression was successfully induced upon removal of the drug and showed a paralleled increase in MPC2 (Fig. 4b). MPC1 overexpressers subjected to TAC-induced hypertrophy had cardiac myocytes with a significantly smaller cross-sectional cell area (Fig. 4c), as well as improved ejection fraction, cardiac output, fractional shortening and attenuated hypertrophic growth compared with *Mhy6tTA* controls (Fig. 4d-e). Metabolomics analysis of MPC1 overexpressers showed a robust and significant increase in citric acid cycle intermediates citrate, aconitate, fumarate and malate, together with a modest increased ATP and adenylate energy charge that would likely to improve cardiac energetics and contribute to their resistance to hypertrophy, consistent with the anticipated increase in mitochondrial pyruvate uptake (Fig. 4f and Supplementary table 2). It is notable that pyruvate, although not statistically significant, was increased in the MPC1 overexpressers. This additional pyruvate could be derived by alanine aminotransferase from alanine, which for reasons that remain elusive, was significantly increased in the overexpresser. Thus, maintaining MPC expression at the levels found in healthy tissue enhanced mitochondrial pyruvate oxidation and limited the maladaptive myocardial growth and progression to heart failure that occurs during stress induced by pressure-overload.

We conclude that MPC abundance determines the extent to which pyruvate is metabolically oxidised in the mitochondria. Decreasing pyruvate flux into myocardial mitochondria leads to metabolic changes that enable hypertrophy, mirroring in part the Warburg Effect that potentiates cancer cell growth. In contrast, potentiating pyruvate flux into myocardial mitochondria leads to metabolic changes that counteract the hypertrophic growth and progression to heart failure. However, the mechanism underling MPC downregulation and consequent metabolic remodelling in the failing heart it is a key question that remains unanswered. Further investigations of the transcriptional regulation and mechano-responsive elements that regulate the expression and activity of the carrier are warranted. A better understanding of these pathways may allow interventions that increase MPC abundance or activity to be identified, which is anticipated to decrease pathogenic hypertrophic growth.

## Methods

### Study approval

This investigation was performed in accordance with the Home Office Guidance on the Operation of the Animals (Scientific Procedures) Act 1986, published by Her Majesty's Stationery Office (London, UK). Animals were maintained humanely in compliance with the "Principles of Laboratory Animal Care" formulated by the National Society for Medical Research and the Guide for Care and Use of Laboratory Animals prepared by the National Academy of Sciences and published by the National Institutes of Health (NIH Pub. No. 85-23, revised 1985). All animal protocols were approved both by the local King's College Ethical Review Process Committee and by the UK Government Home Office (Animals Scientific Procedures Group).

The study was conducted according to Spanish Law for Biomedical Research (Law 14/2007-3 of July) and was compliant with the Declaration of Helsinki. The study and the use of archive samples for this project were approved by the Research Ethics Committee of Galicia. Written, informed consent was obtained from all individuals involved in this study.

### Statistics and Reproducibility

Student's t test for unpaired samples was used to compare experiments comprising two experimental groups with normal distribution and equal variance at one time point. One-way ANOVA followed by a *post hoc* Dunnett's test was used to compare cardiac parameters in experiments with more than 2 groups. Two-way ANOVA followed by a *post hoc* Bonferroni test was used to compare cardiac parameters measured over 21 days in experiments with 2 groups. Statistical analyses were performed using GraphPad Prism 5.0 software. Differences were considered significant at  $P < 0.05$ .

Concomitant loss MPC1 and MPC2 together with a profound increase in cardiac mass was observed consistently for MPC1 KO or MPC2 KO hearts in more than 5 independent experiments.

### Generation of MPC1 and MPC2 conditional knockout with tetO knockin mouse models

Transgenic MPC1 and MPC2 FAST (Flexible Accelerated STOP Tetracycline Operator (tetO)-knock-in) mouse lines were generated by Ingenious Targeting Laboratory (iTL) technologies (Ronkonkoma, New York). Briefly, vectors that contained a LoxP-TetO sequence were inserted immediately upstream of the endogenous ATG initiation site in exon 1 of MPC1 or MPC2 gene sequence. These vectors were independently electroporated into C57BL/6 embryonic stem (ES) cells. ES clones were selected by resistance to neomycin (Neo), screened and microinjected into of blastocysts. Then, blastocysts were implanted into pseudopregnant foster mice. Subsequently, progeny bred with a flippase recombinase (C57BL/6NJ) transgenic mouse to delete the NEO cassette. Identification of germline transmission of the knockout/knock-in and Neo deletion was performed by PCR.

The Ensembl Gene link for the Mpc1 gene was: [http://useast.ensembl.org/Mus\\_musculus/Gene/Summary?](http://useast.ensembl.org/Mus_musculus/Gene/Summary?)

db=core;g=ENSMUSG00000023861;r=17:8282904-8297661;t=ENSMUST00000155364. The FRT-flanked Neo cassette followed by a LoxP site (3' LoxP site) was inserted in intron 1-2 and is about 592 bp away from exon 1. The Neo insertion site was selected to limit interruption of the promoter region. The construct had a long homology arm that extended about 5.83 kb 5' to the 5' LoxP site, and the short homology arm is about 2.3 kb 3' to the FRT-Neo-FRT-LoxP cassette.

The Ensembl Gene link for the Mpc2 gene was: [http://www.ensembl.org/Mus\\_musculus/Gene/Summary?](http://www.ensembl.org/Mus_musculus/Gene/Summary?db=core;g=ENSMUSG00000026568;r=1:165461037-165481214;t=ENSMUST00000027853)

db=core;g=ENSMUSG00000026568;r=1:165461037-165481214;t=ENSMUST00000027853. The MPC2 gene has multiple transcripts and we focused on transcript: Mpc2-001 ENSMUST00000027853. The FRT-flanked Neo cassette followed by a LoxP site (3' LoxP site) was inserted in intron 1-2, which is about 809 bp away from exon 1. The construct was designed such that the long homology arm extends about 5.3 kb 5' to the 5' LoxP site, and the short homology arm is about 2.3 kb 3' from the FRT-Neo-FRT-LoxP cassette.

### Generation of cardiac specific MPC1 and MPC2 knock out and overexpressers

Cardiac specific mouse transgenic lines FVB-Tg(Myh6-cre)2182Mds/J (Jax Labs, stock: 011037) and FVB.Cg-Tg(Myh6-tTA)6Smbf/J (Jax Labs, stock: 003170) were backcrossed for >10 generations into the C57BL/6NJ male mice background (Jax Labs, Stock: 005304). These mice were then crossed with MPC1 or MPC2 FAST transgenic mice to generate cardiac specific MPC KO (*Mhy6CreMPC1* and *Mhy6CreMPC2*) or overexpressers (*Mhy6tTAMPC1* or *Mhy6tTAMPC2*). To aid the understanding and simplify the nomenclature relating to the transgenic mice used in these studies, Mhy6CreMPC1 and Mhy6CreMPC2 mice homozygous for the FAST cassette and heterozygous for Cre cassette were named as MPC1 KO and MPC2 KO. Those mice not containing the FAST cassette that are heterozygous for the Cre cassette were used as controls and named Mhy6Cre. In a similar way, Mhy6CreMPC1 and Mhy6CreMPC2 homozygous for the FAST cassette and heterozygous for tTA cassette were named as MPC1 overexpresser and MPC2 overexpresser. Mice that do not contain the FAST cassette and heterozygous for the tTA cassette were used as controls and named Mhy6tTA. MPC overexpressers and respective tTA controls were fed with a doxycycline diet (TD98186 Envigo, UK) from birth to maintain endogenous expression of the MPC gene. The cardiac specific  $\alpha$ MHC-MerCreMer tamoxifen inducible transgenic line in C57BL/6NJ male mice background was provided by Min Zhang (King's College London, London, UK). These mice were then crossed with MPC1 FAST transgenic mice to generate cardiac specific tamoxifen-inducible MPC1 KO (*Mhy6merCremerMPC1*). *Mhy6merCremerMPC1* homozygous for the FAST cassette and heterozygous for the MerCreMeR cassette were named TAXMPC1. Those mice not containing the FAST cassette and heterozygous for the MerCreMeR cassette were used as controls and named Control-Cre. Intraperitoneal injection (20 mg/kg) of tamoxifen was performed for 5 consecutive days to induce the deletion of the exon 1 of MPC1 and so generate the MPC1 KO. Control-Cre mice were also injected with tamoxifen following the same protocol, which would account for any impact of this drug other than reducing MPC expression.

Unless otherwise stated, male mice between 10-13 weeks of age were used for experiments. Animals were kept under pathogen-free conditions, 12h light–dark cycle, controlled humidity (~40%), temperature (20–22°C), and fed chow and water ad libitum.

### **Transverse aortic constriction and angiotensin II induced hypertrophy**

C57BL/6NJ male mice (body weight  $24 \pm 3$  g, ~12 weeks old) were anaesthetized with isoflurane placed in the supine position under a dissecting microscope. A 5-mm midline incision was performed above the sternal notch to expose the aorta and carotid arteries. The area at both sides of the aorta was cleared and a 7-0 suture was threaded around the aorta between the carotid arteries and tied against a 27 G needle. The needle was then removed, leaving a narrowing of 0.5 mm in diameter. Animals recovered from anesthesia in a 28°C heated chamber. Control, sham operations were performed by doing the same procedure without tying the knot around the aorta. In some studies, hypertrophy was induced by subcutaneous implantation of osmotic minipumps (model 1002; Alzet) for delivery of angiotensin II (Sigma) at an infusion rate of 1 mg/kg/day (23).

Echocardiography was performed with a Vevo 2100 system at heart rates between 400-450 beats per minute using a 40 MHz linear probe (Visualsonics software version 1.0.0, Canada). Mice were anesthetized with 2% isoflurane and the body temperature was maintained at 37 °C. Ejection fraction, stroke volume, and cardiac output were obtained from high-resolution motion-mode images at the level of the papillary muscle using Vevo Software (VisualSonics, software version 1.0.0).

### **Collection of human samples from healthy individuals and patients with hypertrophic cardiomyopathy**

The study was conducted according to Spanish Law for Biomedical Research (Law 14/2007-3 of July) and was compliant with the Declaration of Helsinki. The study and the use of archive samples for this project were approved by the Research Ethics Committee of Galicia. Written, informed consent was obtained from all the individuals involved in this study.

Left ventricle biopsies were obtained from the explanted hearts of patients with hypertrophic cardiomyopathy undergoing cardiac transplantation at the A Coruña Hospital. Hypertrophic cardiomyopathy was defined according to the American College of Cardiology and American Heart Association clinical standards. Left ventricle biopsies of healthy hearts were obtained from unused donor hearts from the A Coruña Hospital following guidelines of Spanish Royal Decrees 2070/1999 and 1301/2006, which regulates the acquisition and use of human tissues for clinical and research purposes. The six individuals with healthy myocardium (2 males and 4 females) had a median age of 52 years. The six patients with hypertrophic cardiomyopathy (3 males and 3 females) had a median age of 52.

### **Immunoblotting analysis**

Reduced protein samples prepared from hearts were separated by SDS-PAGE using the Mini-Protean 3 system (Bio-Rad) and transferred to PDVF membranes (Bio-Rad). Blots were incubated with the following primary antibodies diluted 1:1000 in PBS-Tween 5% milk

overnight: MPC1 (Cell Signalling, #14462), MPC2 (Cell Signalling, #46141) and GAPDH (Cell Signalling, D16H11). One-hour incubation with horseradish peroxidase-coupled anti-rabbit (#7074, Cell Signalling) IgG secondary antibody (diluted 1:1,000 in PBS-Tween 5% milk) together with enhanced chemiluminescence reagent (GE Healthcare) was used to detect primary antibodies bound to the blot. Blots were cut in line with the 25 kDa band, the bottom half was probed for MPC1 or MPC2 and the upper half for GAPDH as a loading control. The densitometry of western blots was performed using Gel Pro Analyzer 3.1 (Media Cybernetics USA).

### Real-time PCR for Cardiac Tissue Samples

A 30 mg sample of cardiac tissue was collected, and RNA was extracted using TRIzol reagent (Invitrogen). Using 2 µg aliquots of RNA, cDNAs were synthesized using the First Strand cDNA synthesis kit (Roche Applied Science, Penzbergh, Germany) with oligo(dT) primers. DNA primers were designed using Primer3' software (version 0.4.0), and sequences were as follows: α-MHC 5'-AGAAGCCCAGCGCTCCCTCA-3' (forward) and 5'-TGCCTCGGG TCAGCTGGGAA-3' (reverse); ANP 5'-TCGCTTGGCCTTTTGGCT-3' (forward) and 5'-TCCAGGTGGTCTAGCAGGTTCT-3' (reverse); β-MHC 5'-CCTCGGGTTAGCTGAGAG ATCA-3' (forward) and 5'-ATGTGCCGGACCTTGGAAG-3' (reverse); BNP 5'-AAG TCCTAGCCAGTCTCCAGA-3' (forward) and 5'-GAGCTGTCTCTGGGCCATTTC-3' (reverse); GAPDH 5'-CATGGCCTTCCGTGTTCCCTA-3' (forward) and 5'-CCTGCTTCA CCACCTTCTTGAT-3' (reverse).

All primers were loaded at 600 nM, and 1 µl of cDNA was amplified by duplicate in 10 µl of 1× SYBR Green Mix (Roche Applied Science, USA), using a ABI7900 HT thermocycler (Thermo Fisher Scientific, USA). The PCR was set up as follows: a denaturing step of 7 min at 94 °C, followed by 35 amplification cycles of 94 °C for 10 s, 60 °C for 10 s, and 72 °C for 10 s. PCR products were tested for melting temperature with a temperature ramp of 2.2 °C/s from 65 to 95 °C and shown to correspond to the expected cloned fragments. GAPDH was used as a reference gene, and relative expression was estimated by the Ct method as the average value of each sample normalized against the average value of control hearts.

### Steady state metabolomics using CE-MS analysis

Approximately 50 mg of frozen tissue was plunged into 1.5 mL of 50% acetonitrile/Milli-Q water containing internal standards (H3304-1002, Human Metabolome Technologies, Inc., Tsuruoka, Japan) at 0°C in order to inactivate enzymes. The tissue was homogenized thrice at 1500 revolutions per minute for 120 s using a tissue homogenizer (Microsmash MS100R, Tomy Digital Biology Co., Ltd., Tokyo, Japan) and then the homogenate was centrifuged at 2300 ×g and 4°C for 5 min. Subsequently, 800 µL of upper aqueous layer was centrifugally filtered through a Millipore 5-kDa cut-off filter at 9100 ×g and 4°C for 120 min to remove proteins. The filtrate was centrifugally concentrated and re-suspended in 50 µL of Milli-Q water for CE-MS analysis.

Metabolome measurements were carried out by Human Metabolome Technologies, Inc., Tsuruoka, Japan. Peaks detected by CE-TOFMS and CE-MS/MS were extracted using

automatic integration software (MasterHands, Keio University, Tsuruoka, Japan and MassHunter Quantitative Analysis B.04.00, Agilent Technologies, Santa Clara, CA, USA, respectively) to obtain peak information including m/z, migration time (MT), and peak area. The peaks were annotated with putative metabolites from the HMT metabolite database based on their MTs in CE and m/z values determined by TOFMS. The tolerance range for the peak annotation was configured at  $\pm 0.5$  min for MT and  $\pm 10$  ppm for m/z. In addition, concentrations of metabolites were calculated by normalizing the peak area of each metabolite with respect to the area of the internal standard and by using standard curves, which were obtained by three-point calibrations.

### C13 flux metabolomics using LC-MS analysis

Approximately 50 mg of frozen heart was grinded in a mortar submerged in liquid nitrogen. Metabolites were extracted using a solution with 50% methanol, 20% acetonitrile and 30% H<sub>2</sub>O. LC-MS analysis of the extracted samples was performed using a Q Exactive Hybrid Quadrupole-Orbitrap mass spectrometer coupled to a Vanquish UHPLC system (Thermo Fisher Scientific). The liquid chromatography system was fitted with a Sequant ZIC-pHILIC column (150 mm  $\times$  2.1 mm) and guard column (20 mm  $\times$  2.1 mm) from Merck Millipore (Germany) and temperature maintained at 35°C. The mobile phase was composed of 10 mM ammonium carbonate and 0.1% ammonium hydroxide in water (solvent A), and acetonitrile (solvent B). The flow rate was set at 100  $\mu$ L/min with the gradient described previously (Mackay et al., 2015). The mass spectrometer was operated in full MS and polarity switching mode. The acquired spectra were analyzed using XCalibur Qual Browser and XCalibur Quan Browser software 4.2 (Thermo Scientific)

### Dystrophin Immunohistochemistry

Heart tissues were fixed in 4% formalin/PBS and embedded in paraffin using an ASP300S dehydration machine (Leica, Wetzlar, Germany) and an EG1160 tissue embedding system (Leica, Wetzlar, Germany). Immuno-histochemical staining was performed as follows: Sections were cut at a thickness of 2  $\mu$ m. After dewaxing and inactivation of endogenous peroxidases (PBS/3% hydrogen peroxide), antibody-specific heat mediated antigen retrieval was performed using the Ventana Benchmark XT machine (Ventana, Tuscon, Arizona, USA). Sections were blocked (PBS/10% FCS) and afterwards incubated with anti-dystrophin antibody (1:200; MAB1645, EMD Millipore). For detection of specific binding, the Ultra View Universal DAB Detection Kit (Ventana, Roche) was used that contains secondary antibodies, DAB stain and counter staining reagent for detection of nuclei. Representative images were taken with a Leica DMD108 digital microscope. Cardiomyocyte area quantification was analysed using ImageJ (version 1.51W).

### NADP/NADPH and NAD/NADH assay

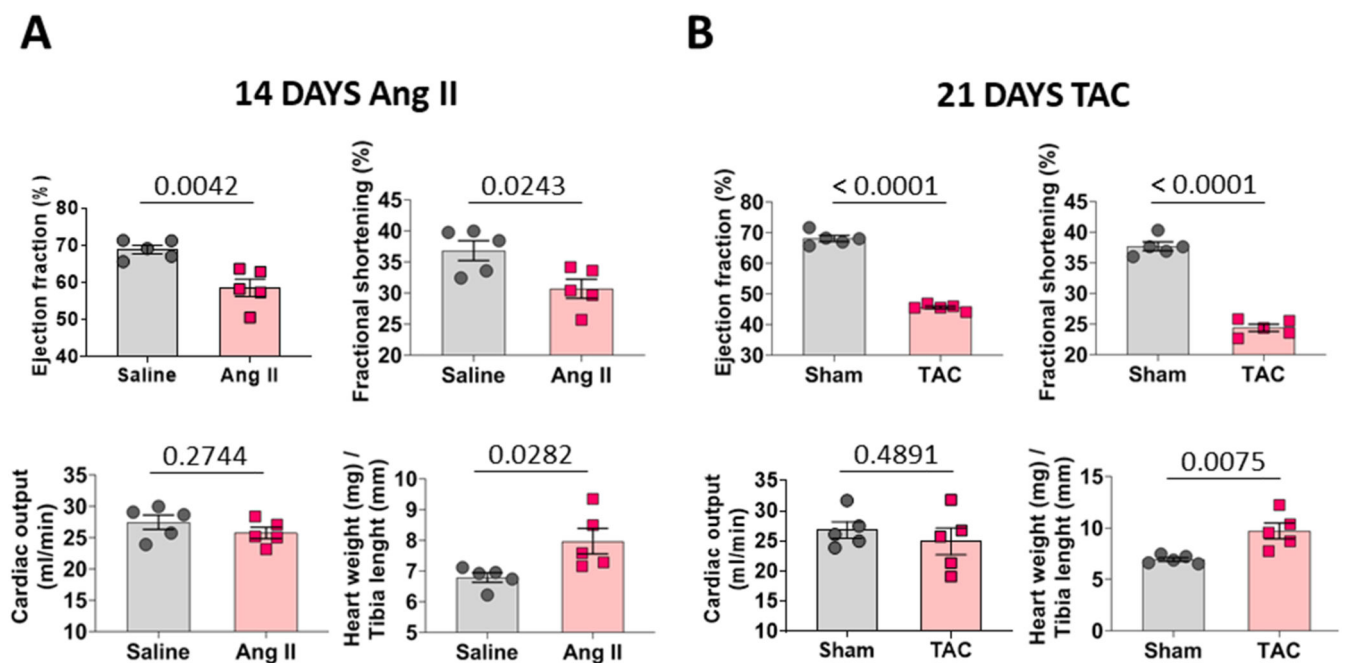
NADP<sup>+</sup>/NADPH and NAD/NADH ratios were measured using the NADP<sup>+</sup>/NADPH-GLO and NAD<sup>+</sup>/NADH assay kit (Promega) respectively following the manufacturer's instructions. Briefly, 5  $\times$  10<sup>6</sup> H9C2 cells or 30 mg of heart tissue were lysed in 200  $\mu$ l or 300  $\mu$ l respectively of base solution (Sigma). Half of the lysate was treated with 0.4 N HCl at 60 °C in order to remove the NADH and NADPH to allow measurement of NAD<sup>+</sup> and NADP<sup>+</sup>.

Cell and tissue lysates were mixed with kit detection reagents and after 30 min, NADP<sup>+</sup>/NADPH ratios were measured using CLARIOstar® Plus (BMG, Labtech).

### Real-time cell proliferation analysis

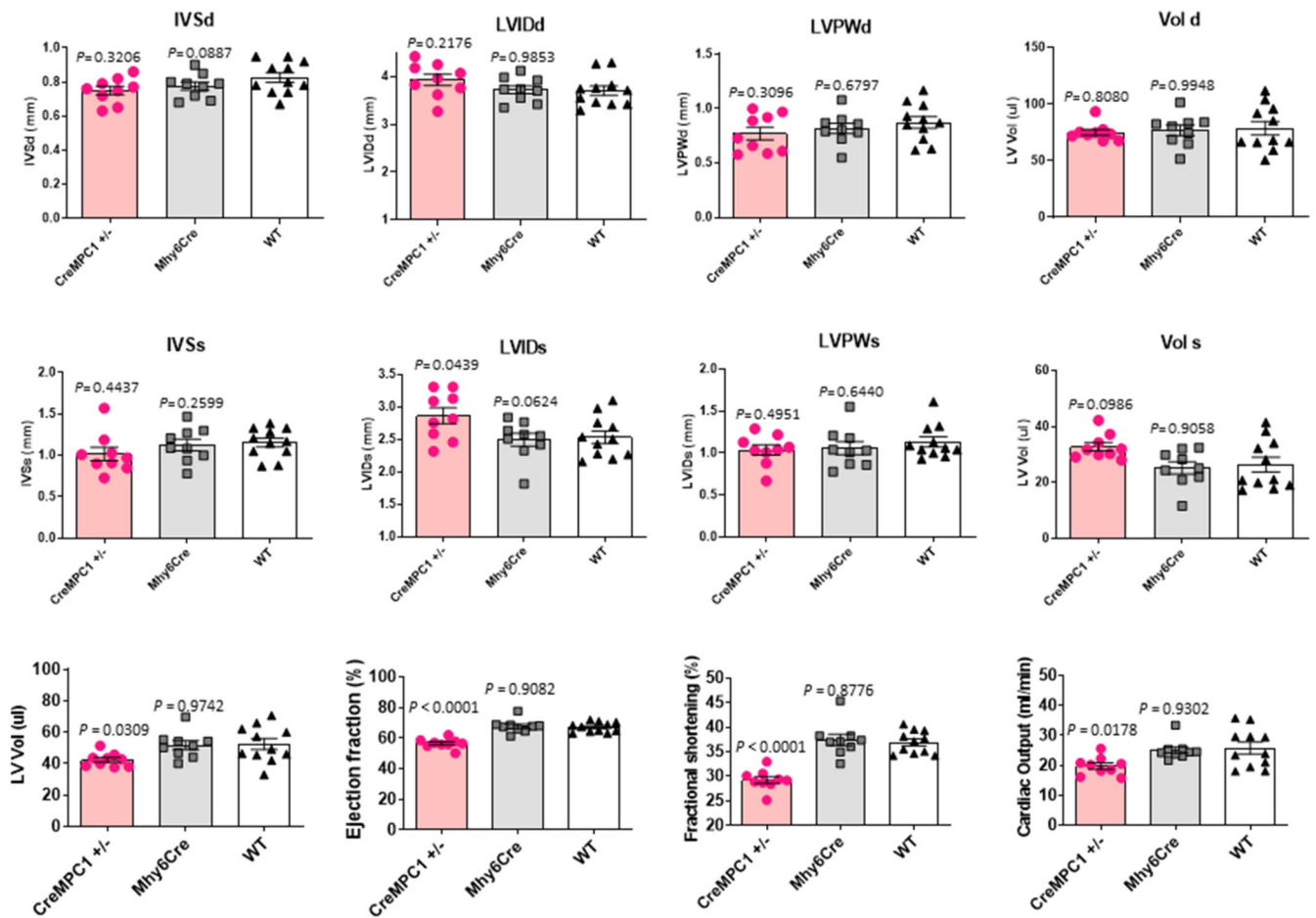
The xCELLigence system (Acea Biosciences, RTCA SP) was used for real-time and time-dependent analysis of H9C2 cell responses to UK5099 (10  $\mu$ M or 20  $\mu$ M). 20,000 cells were seeded on an PET 16 E-Plate and cultured in 250  $\mu$ l of Dulbecco's Modified Eagle Glutamax Medium (Thermo Fisher Scientific). After 24 hours, cells were treated with vehicle or UK5099 and real-time cell index was continuously measured for the following 96 hours using the cell impedance detection system. Cell Index is a measure of impedance which correlates with the number, attachment and size of the cells.

### Extended Data



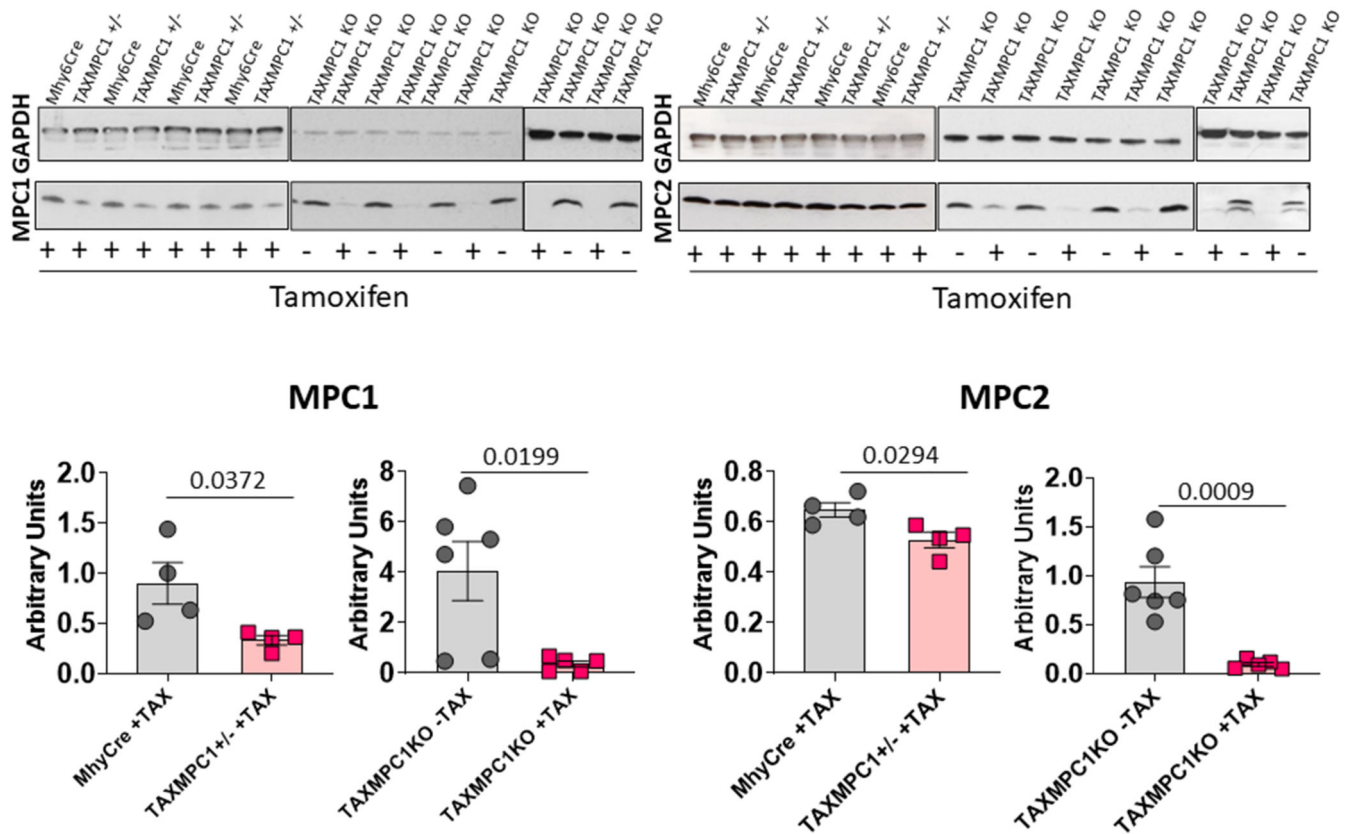
**Extended Data Fig. 1.**

**a**, Cardiac function of wild type mice injected with saline or angiotensin presented as ejection fraction, fractional shortening, cardiac output and stroke volume. Development of cardiac hypertrophy was indexed by the heart weight/tibia length ratio (n= 5 mice/group). **b**, Cardiac function of wild type mice subjected to a sham or thoracic aortic constriction operation presented as ejection fraction, fractional shortening, cardiac output and stroke volume. Development of cardiac hypertrophy was indexed by the heart weight/tibia length ratio (n= 5 mice/group). All statistical significances ( $P < 0.05$ ) were calculated using unpaired, two-tailed, Student's t-tests. Data are presented as mean  $\pm$  S.E.M.



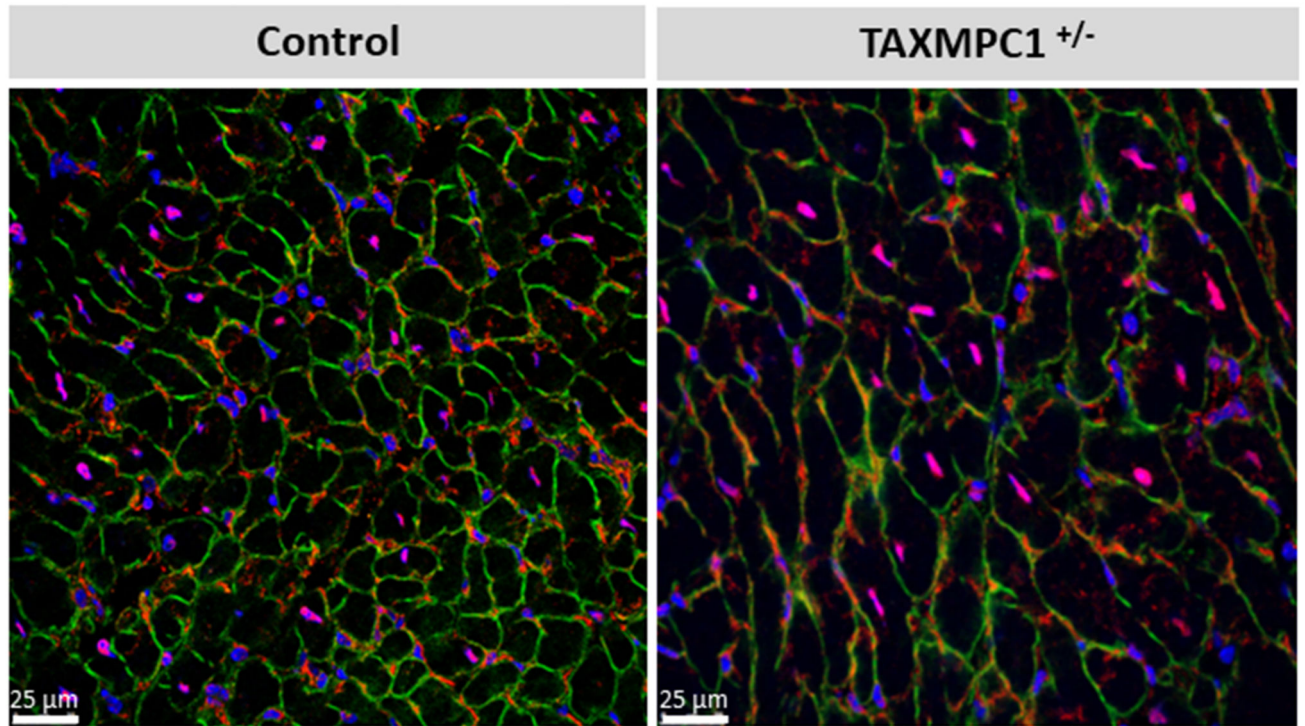
### Extended Data Fig. 2.

Cardiac function of partial MPC1 KO ( $-/+$  CreMPC1), Mhy6Cre control and wild type mice was indexed using echocardiography. Cardiac function is presented as interventricular septum thickness at end-diastole and end systole (IVSd and IVSs), left ventricular internal-diastolic (LVIDd), internal-systolic dimension (LVIDs), left ventricular posterior wall in diastole and systole (LVPWd and LVPWs), end diastolic and end systolic volume (Vol d and Vol s), stroke volume, ejection fraction, and fractional shortening ( $n=9-10$  mice/group). Statistical significances ( $P < 0.05$ ) were calculated using one-way ANOVA adjusted using Dunnett's test for multiple comparisons. Data are presented as mean  $\pm$  S.E.M.



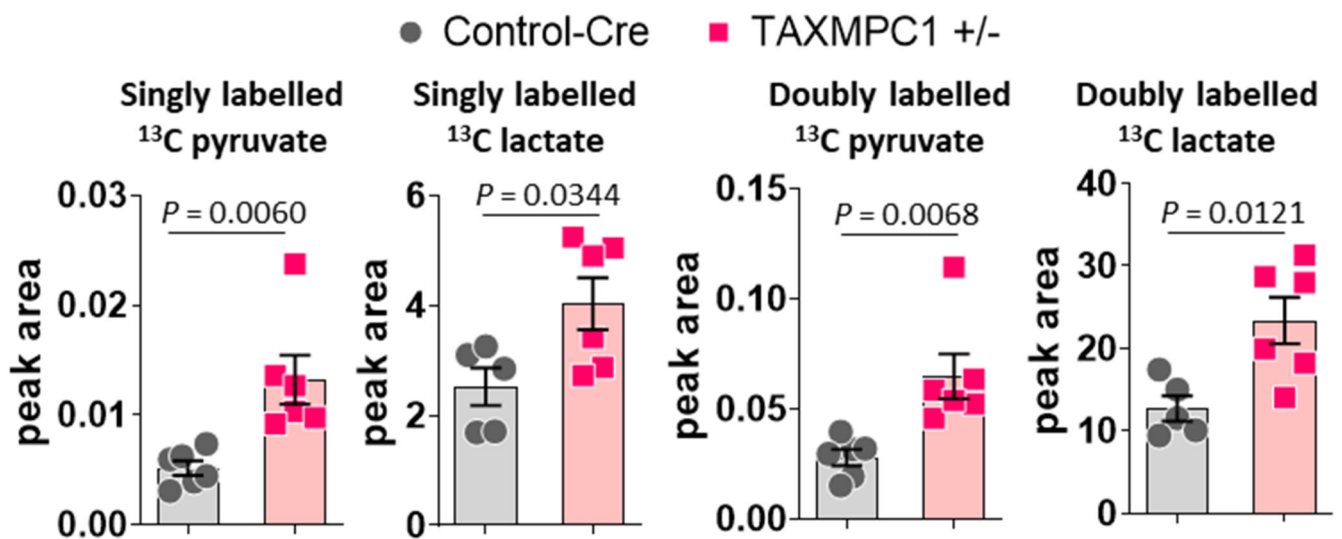
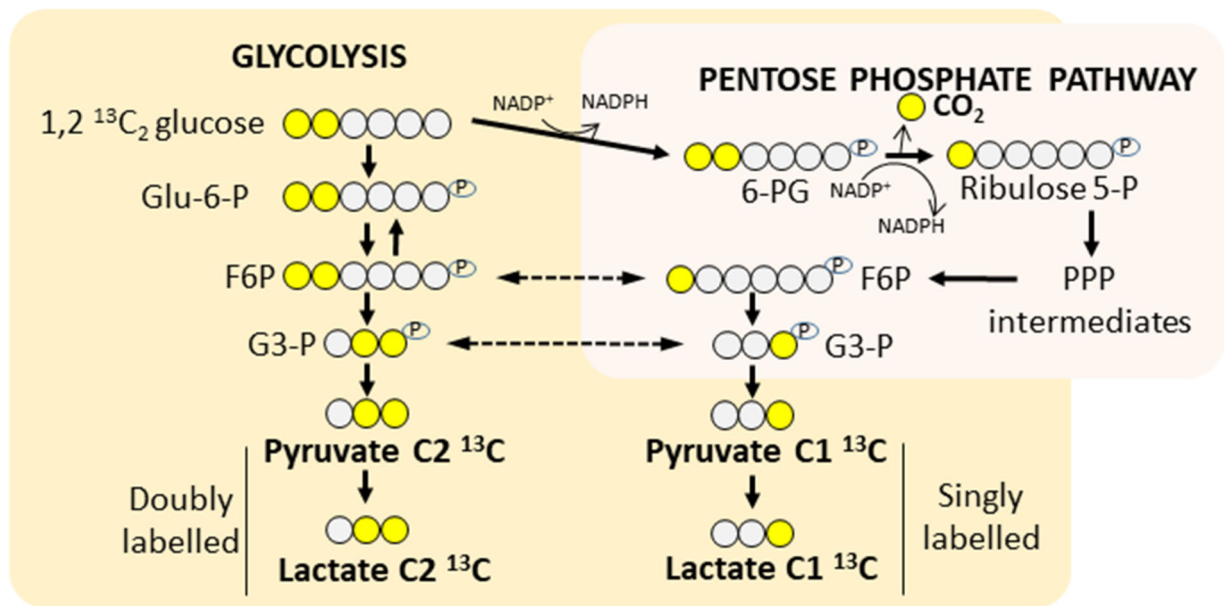
**Extended Data Fig. 3.**

Western immunoblotting analysis of homozygous (TAXMPC1 KO) or heterozygous (TAXMPC1<sup>+/-</sup>) mouse hearts showed that tamoxifen injection to 8-week-old transgenic TAXMPC1 adults promoted a significant reduction in MPC1 and MPC2 protein abundance (n= 4-6 biologically independent heart samples/group). All statistical significances (P < 0.05) were calculated using unpaired, two-tailed, Student's t-tests. Data are presented as mean ± S.E.M.



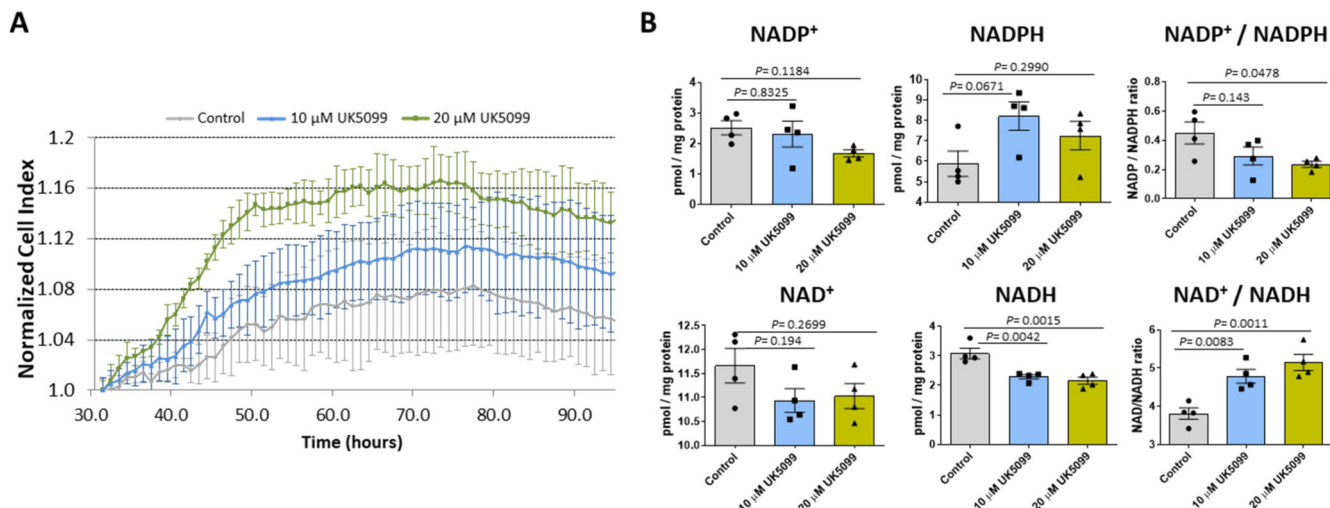
**Extended Data Fig. 4.**

Immunofluorescence analysis of dystrophin (green), MPC1 (red) and DAPI enabled measurement of cardiomyocyte cross-sectional area. TAXMPC1<sup>+/-</sup>, which are characterised by partial knockout of MPC expression, were hypertrophic as evidenced by the presence of larger cells. (Scale bar represents 25  $\mu\text{m}$ ). Representative image for n= 3 biologically independent hearts/group.



Extended Data Fig. 5.

Diagram adapted from Carpenter et al.<sup>31</sup> to show measurement of flux towards the PPP. TAXMPC1<sup>+/-</sup> hearts presented an increase in doubly and singly labelled <sup>13</sup>C lactate and pyruvate (n= 5-6 biologically independent heart samples/group). Peak area was normalized by HEPES. All statistical significances ( $P < 0.05$ ) were calculated using unpaired, two-tailed, Student's t-tests. Data are presented as mean  $\pm$  S.E.M.



### Extended Data Fig. 6.

**a**, Proliferation and growth of H9C2 cells was increased in response to the mitochondrial pyruvate carrier inhibitor UK5099 (10  $\mu$ M or 20  $\mu$ M). **b**, H9C2 cells treated with 20  $\mu$ M UK5099 showed a significant reduction in NADP/NADPH and NAD/NADH ratios, whereas only the NAD/NADH ratio was significant in H9C2 cells treated with 10  $\mu$ M UK5099 ( $n = 4$  biologically independent cell samples/group). Statistical significances ( $P < 0.05$ ) were calculated using one-way ANOVA adjusted using Dunnett's test for multiple comparisons. Data are presented as mean  $\pm$  S.E.M.

## Supplementary Material

Refer to Web version on PubMed Central for supplementary material.

## Acknowledgements

This work was supported by the British Heart Foundation, the European Research Council (ERC Advanced award), and the Medical Research Council. PE is supported by The Barts Charity Cardiovascular Programme Award G00913. We also thank Kristin Hartmann for her technical assistance and Biobank of "A Coruña" (XXIAC-Instituto de Investigación Biomédica de A Coruña) for providing us healthy heart tissue samples. TE acknowledges support from NIHR Biomedical Research Centre at Guy's and St Thomas' NHS Foundation Trust and KCL; the Centre of Excellence in Medical Engineering funded by the Wellcome Trust and EPSRC (WT 088641/Z/09/Z) and the KCL Comprehensive Cancer Imaging Centre funded by the Cancer Research UK (CRUK) and EPSRC in association with MRC and DoH.

## Data availability

The data that support the findings of this study are available from the corresponding author on request. Human Metabolome Technologies uses the Human Metabome Database (HMDB) (<https://hmdb.ca/>). The metabolomic data and the HMDB link for each metabolite is available online as Supplementary Table 1 and Supplementary Table 2. Source data for Figs. 1-4 and Supplementary Figs. 1-3 and 5 and 6 are available online.

The Ensembl Gene link used for the generation of MPC1 conditional knockout with tetO knockin is: [http://useast.ensembl.org/Mus\\_musculus/Gene/Summary?db=core;g=ENSMUSG00000023861;r=17:8282904-8297661;t=ENSMUST00000155364](http://useast.ensembl.org/Mus_musculus/Gene/Summary?db=core;g=ENSMUSG00000023861;r=17:8282904-8297661;t=ENSMUST00000155364)

The Ensembl Gene link used for the generation of MPC2 conditional knockout with tetO knockin is: [http://www.ensembl.org/Mus\\_musculus/Gene/Summary?db=core;g=ENSMUSG00000026568;r=1:165461037-165481214;t=ENSMUST00000027853](http://www.ensembl.org/Mus_musculus/Gene/Summary?db=core;g=ENSMUSG00000026568;r=1:165461037-165481214;t=ENSMUST00000027853)

## References

1. Lopaschuk GD, Belke DD, Gamble J, Itoi T, Schonekess BO. Regulation of fatty acid oxidation in the mammalian heart in health and disease. *Biochimica et biophysica acta*. 1994; 1213:263–276. [PubMed: 8049240]
2. Kerr PM, Suleiman MS, Halestrap AP. Reversal of permeability transition during recovery of hearts from ischemia and its enhancement by pyruvate. *The American journal of physiology*. 1999; 276:H496–502. [PubMed: 9950850]
3. Barger PM, Kelly DP. Fatty acid utilization in the hypertrophied and failing heart: molecular regulatory mechanisms. *The American journal of the medical sciences*. 1999; 318:36–42. [PubMed: 10408759]
4. Razeghi P, et al. Metabolic gene expression in fetal and failing human heart. *Circulation*. 2001; 104:2923–2931. [PubMed: 11739307]
5. Oliver MF, Kurien VA, Greenwood TW. Relation between serum-free-fatty acids and arrhythmias and death after acute myocardial infarction. *Lancet*. 1968; 1:710–714. [PubMed: 4170959]
6. Jung WI, et al. 31P NMR spectroscopy detects metabolic abnormalities in asymptomatic patients with hypertrophic cardiomyopathy. *Circulation*. 1998; 97:2536–2542. [PubMed: 9657474]
7. Nascimben L, et al. Mechanisms for increased glycolysis in the hypertrophied rat heart. *Hypertension*. 2004; 44:662–667. [PubMed: 15466668]
8. Kagaya Y, et al. Effects of long-term pressure overload on regional myocardial glucose and free fatty acid uptake in rats. A quantitative autoradiographic study. *Circulation*. 1990; 81:1353–1361. [PubMed: 2180593]
9. Kolwicz SC Jr, Tian R. Glucose metabolism and cardiac hypertrophy. *Cardiovascular research*. 2011; 90:194–201. [PubMed: 21502371]
10. Allard MF, Schonekess BO, Henning SL, English DR, Lopaschuk GD. Contribution of oxidative metabolism and glycolysis to ATP production in hypertrophied hearts. *The American journal of physiology*. 1994; 267:H742–750. [PubMed: 8067430]
11. Sorokina N, et al. Recruitment of compensatory pathways to sustain oxidative flux with reduced carnitine palmitoyltransferase I activity characterizes inefficiency in energy metabolism in hypertrophied hearts. *Circulation*. 2007; 115:2033–2041. [PubMed: 17404155]
12. Taegtmeier H, Overturf ML. Effects of moderate hypertension on cardiac function and metabolism in the rabbit. *Hypertension*. 1988; 11:416–426. [PubMed: 3366475]
13. Smith SH, Kramer MF, Reis I, Bishop SP, Ingwall JS. Regional changes in creatine kinase and myocyte size in hypertensive and nonhypertensive cardiac hypertrophy. *Circulation research*. 1990; 67:1334–1344. [PubMed: 2147129]
14. Bricker DK, et al. A mitochondrial pyruvate carrier required for pyruvate uptake in yeast, *Drosophila*, and humans. *Science*. 2012; 337:96–100. [PubMed: 22628558]
15. Herzig S, et al. Identification and functional expression of the mitochondrial pyruvate carrier. *Science*. 2012; 337:93–96. [PubMed: 22628554]
16. Schell JC, et al. Control of intestinal stem cell function and proliferation by mitochondrial pyruvate metabolism. *Nature cell biology*. 2017; 19:1027–1036. [PubMed: 28812582]
17. Flores A, et al. Lactate dehydrogenase activity drives hair follicle stem cell activation. *Nature cell biology*. 2017; 19:1017–1026. [PubMed: 28812580]

18. Zhong Y, et al. Application of mitochondrial pyruvate carrier blocker UK5099 creates metabolic reprogram and greater stem-like properties in LnCap prostate cancer cells in vitro. *Oncotarget*. 2015; 6:37758–37769. [PubMed: 26413751]
19. Li X, et al. Mitochondrial pyruvate carrier function determines cell stemness and metabolic reprogramming in cancer cells. *Oncotarget*. 2017; 8:46363–46380. [PubMed: 28624784]
20. Schell JC, et al. A role for the mitochondrial pyruvate carrier as a repressor of the Warburg effect and colon cancer cell growth. *Molecular cell*. 2014; 56:400–413. [PubMed: 25458841]
21. Li X, et al. MPC1 and MPC2 expressions are associated with favorable clinical outcomes in prostate cancer. *BMC cancer*. 2016; 16:894. [PubMed: 27852261]
22. Xiao B, et al. Downregulation of COUP-TFII inhibits glioblastoma growth via targeting MPC1. *Oncology letters*. 2018; 15:9697–9702. [PubMed: 29928345]
23. Gray LR, et al. Hepatic Mitochondrial Pyruvate Carrier 1 Is Required for Efficient Regulation of Gluconeogenesis and Whole-Body Glucose Homeostasis. *Cell metabolism*. 2015; 22:669–681. [PubMed: 26344103]
24. El Alaoui-Talibi Z, Guendouz A, Moravec M, Moravec J. Control of oxidative metabolism in volume-overloaded rat hearts: effect of propionyl-L-carnitine. *The American journal of physiology*. 1997; 272:H1615–1624. [PubMed: 9139943]
25. Wambolt RB, et al. Glucose utilization and glycogen turnover are accelerated in hypertrophied rat hearts during severe low-flow ischemia. *Journal of molecular and cellular cardiology*. 1999; 31:493–502. [PubMed: 10198181]
26. Zimmer HG. Regulation of and intervention into the oxidative pentose phosphate pathway and adenine nucleotide metabolism in the heart. *Molecular and cellular biochemistry*. 1996; 160–161:101–109.
27. Gupte SA, et al. Glucose-6-phosphate dehydrogenase-derived NADPH fuels superoxide production in the failing heart. *Journal of molecular and cellular cardiology*. 2006; 41:340–349. [PubMed: 16828794]
28. Hildyard JC, Ammala C, Dukes ID, Thomson SA, Halestrap AP. Identification and characterisation of a new class of highly specific and potent inhibitors of the mitochondrial pyruvate carrier. *Biochimica et biophysica acta*. 2005; 1707:221–230. [PubMed: 15863100]
29. Fernandez-Caggiano M, et al. Analysis of Mitochondrial Proteins in the Surviving Myocardium after Ischemia Identifies Mitochondrial Pyruvate Carrier Expression as Possible Mediator of Tissue Viability. *Mol Cell Proteomics*. 2016; 15:246–255. [PubMed: 26582072]
30. van Bilsen M, van Nieuwenhoven FA, van der Vusse GJ. Metabolic remodelling of the failing heart: beneficial or detrimental? *Cardiovascular research*. 2009; 81:420–428. [PubMed: 18854380]
31. Carpenter KL, et al. (13)C-labelled microdialysis studies of cerebral metabolism in TBI patients. *Eur J Pharm Sci*. 2014; 57:87–97. [PubMed: 24361470]

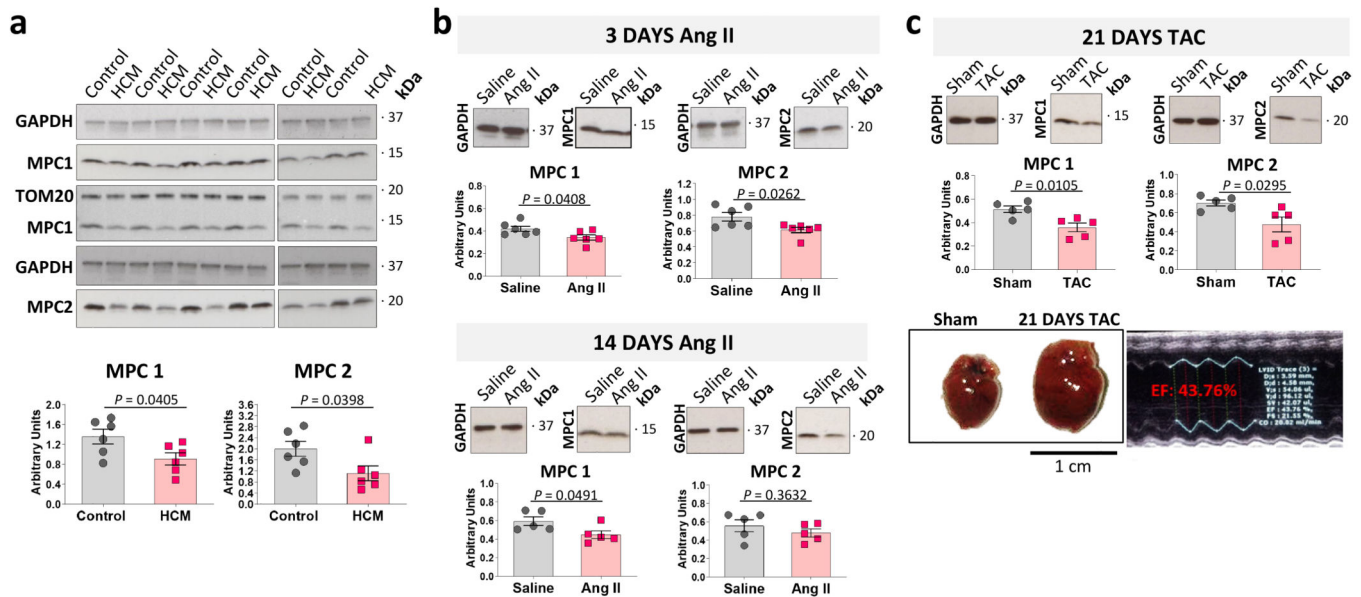


**Figure 1. MPC1 and MPC2 abundance is lower in hearts of patients with hypertrophic cardiomyopathy and mice induced to undergo pathological hypertrophy.**

**a.** Quantitative western immunoblotting analysis showed MPC1 and MPC2 were significantly less abundant in myocardium from patients with hypertrophic cardiomyopathy (HCM) compared with those from donors with a healthy heart (Control), as normalised to GAPDH expression. TOM20 was included as a mitochondrial loading marker control. (n= 6 biologically independent heart samples/group). **b.** Quantitative western immunoblotting analysis showed 3-days of angiotensin II treatment promoted significant loss of cardiac MPC1 as normalised to GAPDH (n= 6 biologically independent heart samples/group). Cardiac MPC1 and MPC2 remained lower 14-days after exposure to angiotensin II, as normalised to GAPDH expression (n= 5 biologically independent heart samples/group). **c.** Quantitative western immunoblotting analysis, normalised to GAPDH expression, showed MPC1 and MPC2 were significantly reduced in hearts from mice 21-days after they were subjected to transverse-aortic constriction compared to sham II controls in which growth was not promoted (n= 5 biologically independent heart samples/group). The transverse-aortic constriction procedure that decreased MPC1/2 expression also increased hypertrophic growth as evidenced by a significant increase in heart weight/tibia length ratio, compared with the sham group. Statistical significances ( $P < 0.05$ ) were calculated using unpaired, two-tailed, Student's t-tests. Data are presented as mean  $\pm$  S.E.M.

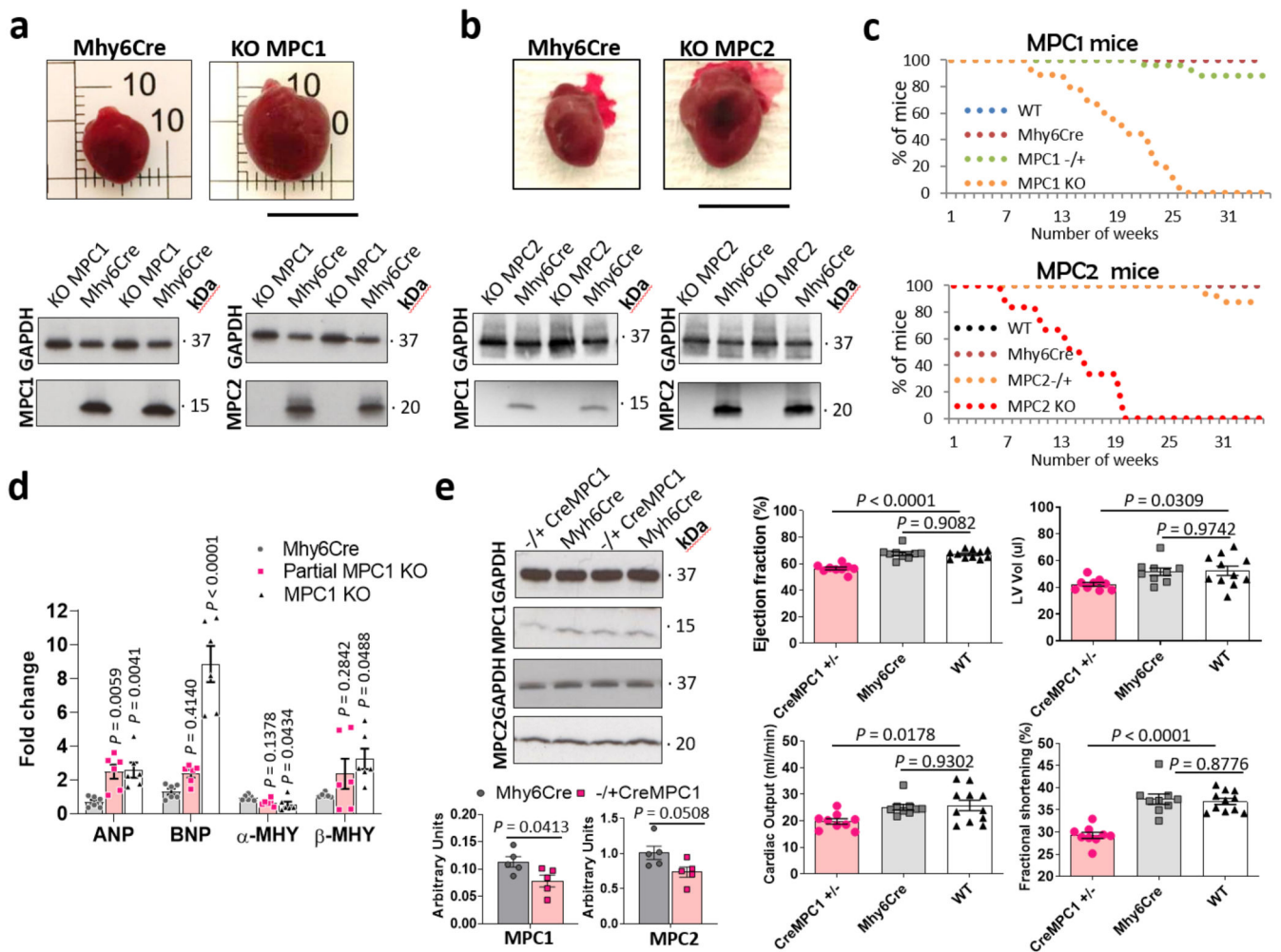


**Figure 2. MPC1 or MPC2 knock out from birth induces heart hypertrophy and increases mortality.**

**a,b,** Quantitative western immunoblotting analysis showed MPC1 KO or MPC2 KO hearts showed a reciprocal, concomitant loss of the other subunit of the carrier. This loss of MPC1/2 was associated with a profound increase in cardiac mass. **c,** MPC1 or MPC2 KO mice, in which the MPC gene was deleted from birth, showed enhanced mortality compared with Mhy6Cre control mice as illustrated by the Kaplan-Meier survival curves, probably because of cardiac failure (n= 12-20 mice/group). **d,** Real-time PCR analysis showed both the partial MPC1 and MPC1 KO hearts also has significantly increased levels of mRNA hypertrophic markers, namely atrial natriuretic peptide (ANP) and brain natriuretic peptide (BNP), whereas  $\beta$ -myosin heavy chain  $\beta$ -MHC was only significantly increased in MPC1 KO hearts (n= 5 biologically independent heart samples/group). Statistical significances ( $P < 0.05$ ) were calculated using one-way ANOVA adjusted using Dunnett's test for multiple comparisons. **e,** Partial MPC1 KO (-/+ *CreMPC1*) showed lower expression of MPC1 and MPC2 subunits that was comparable to that in angiotensin II- or transverse-aortic constriction-induced hypertrophic hearts. The partial MPC1 KO mice were hypertrophic, exhibited a reduced ejection fraction, left ventricular volume (LV Vol) and fractional

shortening (n= 9-10 mice/group). Statistical significances ( $P < 0.05$ ) were calculated using unpaired, two-tailed, Student's t-tests and one-way ANOVA adjusted using Dunnett's test for multiple comparisons. Data are presented as mean  $\pm$  S.E.M.

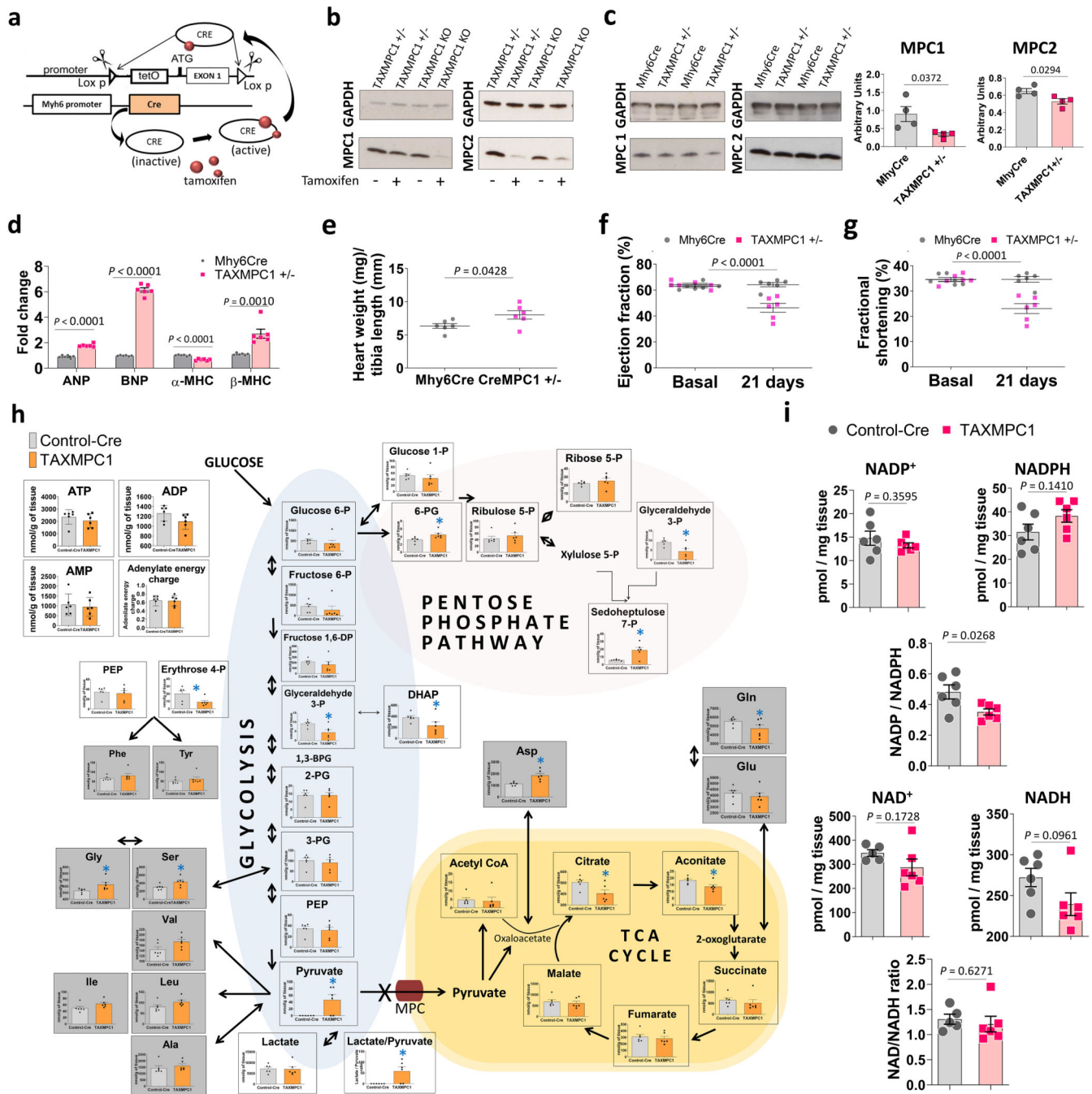


**Figure 3. Inducibly decreasing MPC expression in adult mice switches metabolism to an anabolic programme that causes hypertrophic growth.**

**a.** Design rationale for cardiomyocyte-specific tamoxifen-inducible KO (TAXMPC1) transgenic mice. Intraperitoneal administration of tamoxifen to adult transgenic mice activates Cre recombinase with the consequent excision of first exon of the MPC1 gene only in cardiomyocytes. **b.** Western immunoblotting analysis of homozygous (TAXMPC1 KO) or heterozygous (TAXMPC1<sup>+/-</sup>) mouse hearts showed that tamoxifen injection to 8-week-old transgenic TAXMPC1 adults promoted a significant reduction in MPC1 and MPC2 protein

abundance. **c-d**, Western immunoblotting analysis of heart sections from TAXMPC1<sup>+/-</sup> mice confirmed the anticipated partial reduction in MPC subunit expression 21-days after MPC was inducibly downregulated with tamoxifen (n= 4 biologically independent heart samples/group). This hypertrophy was corroborated by increases in the mRNA hypertrophic markers atrial natriuretic peptide (ANP), brain natriuretic peptide (BNP) and  $\beta$ -myosin heavy chain ( $\beta$ -MHC) in the same samples (n= 5 biologically independent heart samples/group). **e-g**, Partial MPC knockdown also increased hypertrophy, as indexed by the heart weight/tibia length ratio, resulting in left ventricular dysfunction characterised by decreases in ejection fraction and fractional shortening (n= 5 mice/group). **h**, Pathway analysis obtained from mass spectrometry-based metabolomics of TAXMPC1 KO hearts showed a significant reduction in citric acid cycle intermediates citrate and aconitate, with a corresponding significant increase in pentose phosphate pathway (PPP) metabolites 6-phosphogluconic acid and 7-sepdoheptulose phosphate (n= 5 biologically independent heart samples/group). **i**, TAXMPC1 KO hearts showed a significant reduction in the ratio NADP/NADPH, whereas there was no difference in the NAD/NADH ratio (n= 5-6 biologically independent heart samples/group). All statistical significances (\*P < 0.05) were calculated using unpaired, two-tailed, Student's t-tests. Data are presented as mean  $\pm$  S.E.M.

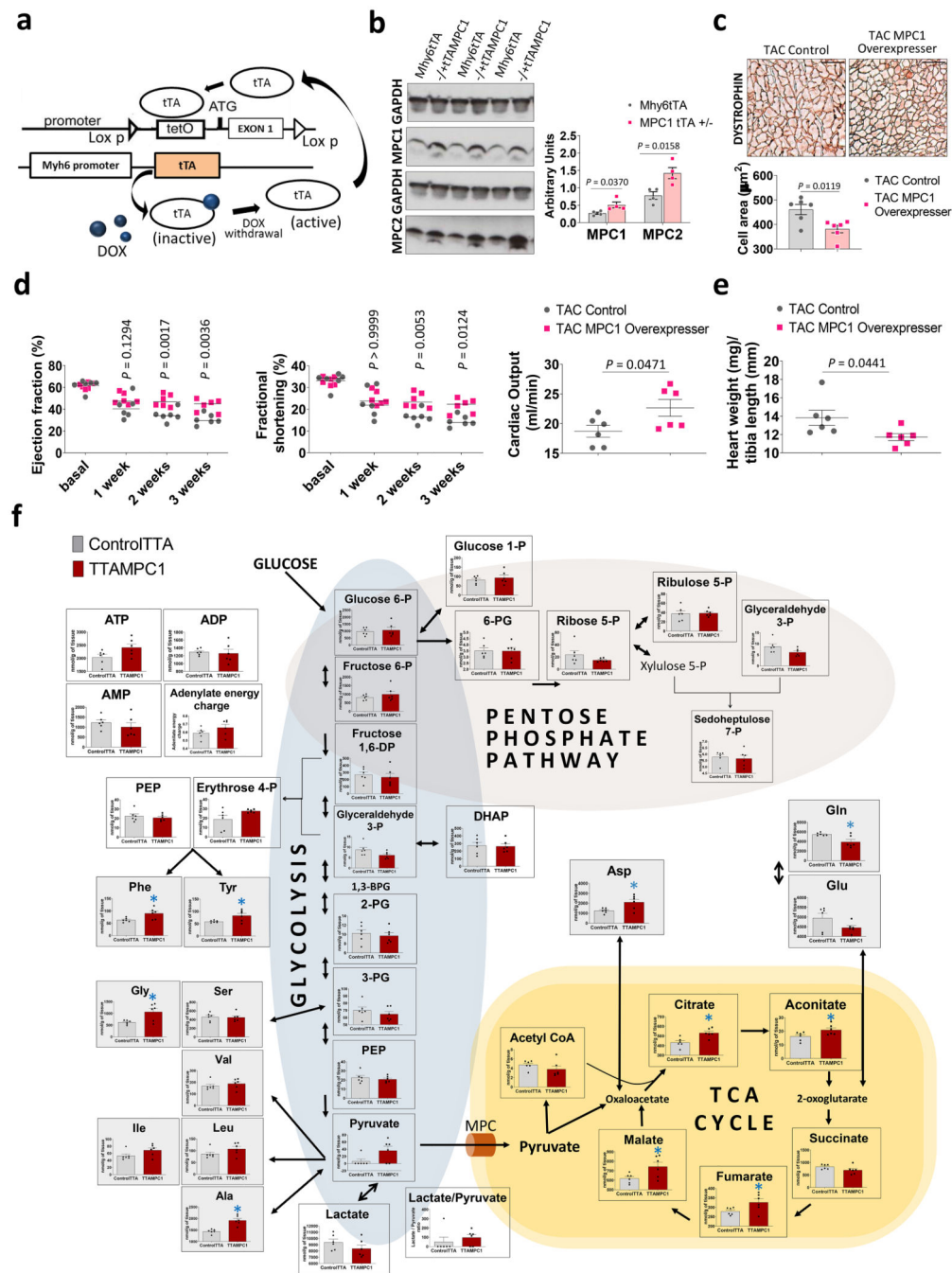


**Figure 4. Conserved MPC expression in MPC1 overexpressors in a TAC model of cardiac hypertrophy is cardioprotective and limits aberrant growth.**

**a.** Overview of the design rationale for inducible cardiomyocyte-specific overexpression of MPC1 (tAMPC1) or MPC2 (tAMPC2) transgenic mice. Tetracycline controlled *trans*-activator protein (tTA) is inactive in the presence of doxycycline, however the withdrawal of this drug induces an efficient interaction between tTA and the tetO promoter which should promote enhanced MPC1 or MPC2 transcription. **b.** Western immunoblotting analysis of hearts from tAMPC1 mice showed increased MPC1 and MPC2 expression compared to the

*Mhy6tTA* control 21 days after doxycycline withdrawal (n= 4 biologically independent heart samples/group). **c**, Histological measurement of cardiomyocyte surface area in heart tissue sections by immunostaining with dystrophin showed MPC1 overexpression reduced cardiomyocyte size compared to *Mhy6tTA* controls in mice subjected to TAC (n= 150-200 cells examined over 6 independent heart samples per group. Scale bar represents 100  $\mu\text{m}$ ). **d**, Echocardiography analysis performed over 3 consecutive weeks following TAC-induced hypertrophy showed a higher ejection fraction and fractional shortening from week 2 in mice induced to overexpress MPC1 compared to *Mhy6tTA* controls. Cardiac output was also significantly better than controls in MPC1 overexpressers 3 weeks after TAC-induced hypertrophy (n= 5-6 mice/group). **e**, Indeed, hypertrophy as indexed by heart weight/tibia length ratio was significantly lower in MPC1 overexpressers compared to control expressing normal levels of the carrier (n= 5-6 mice/group). **f**, Pathway analysis obtained from mass spectrometry-based metabolomics showed that MPC1 overexpressers significantly increased citric acid cycle intermediates, including citric acid, aconitate, fumarate and malate (n= 6 biologically independent heart samples/group). Statistical significances (\* $P < 0.05$ ) were calculated using unpaired, two-tailed, Student's t-tests for figures 4e, 4c, cardiac output graph in 4d and 4e. Two-way ANOVA adjusted by Bonferroni's multiple comparisons test was used for figure 4d. Data are presented as mean  $\pm$  S.E.M.